Modulation by NPYR underlies experience-dependent, sexually dimorphic learning

Sonu Peedikayil-Kurien[1,2], Rizwanul Haque[1,2], Asaf Gat[1,2] and Meital Oren-Suissa[1,2*]

[1] Department of Brain Sciences, Weizmann Institute of Science; Rehovot, 7610001, Israel.

[2]Department of Molecular Neuroscience, Weizmann Institute of Science, Rehovot 7610001, Israel

*Corresponding author. Email: meital.oren@weizmann.ac.il

Abstract: The evolutionary paths taken by each sex within a given species sometimes diverge, resulting in behavioral differences that promote specific fitness outcomes for each sex. Given their distinct needs, the mechanism by which each sex learns from a shared experience is still an open question. We reveal a novel sexual dimorphism in learning: *C. elegans* males do not learn to avoid the pathogenic bacteria PA14 as efficiently and rapidly as hermaphrodites, even though their innate immunity recognizes the pathogen in a similar manner. Notably, we observe sexually dimorphic neuronal activity following pathogen exposure: hermaphrodites generate robust representations while males, in line with their behavior, exhibit contrasting representations, suggesting that a mechanism that modulates incoming sensory cues is at play. Transcriptomic and behavioral analysis revealed that the neuropeptide receptor *npr-5*, an ortholog of the mammalian NPY receptor, regulates male learning by modulating neuronal activity. Furthermore, we show the dependency of the males' decision-making phenotype on their sexual status and demonstrate the pivotal role of *npr-5* in this regulation as a 'sensory gatekeeper'. Thus, collectively, we portray sex-specific plasticity in behavior toward a shared experience by modulating learning to fulfill the evolutionary needs.

Main Text:

Learning facilitates the organism's ability to cope with a changing environment, making it an inherent property of biological neural systems[1]. To adapt to the environment, the organism needs to retain the learning experience and then use the stored information to alter future responses[2]. The synaptic basis of learning and memory has been well established and provides a solid foundation to assess the relationship between experience-dependent learning and survival[3].

Since sexual selection predicts that males and females are subjected to different selection pressures leading to dimorphisms[4,5], it goes to reason that the same would occur for an essential ability such as learning. Consistent with this prediction, several sex-shared traits such as perception and learning have been previously demonstrated to be modulated by the genetic sex[6–12]. It has also been proposed that context-dependent learning by itself can influence the predicted evolutionary outcome[13]. Thus, sex-specific evolutionary drives might be in tension with decision-making processes when facing an environmental cue[14,15]. While a significant portion of sex differences in behavior could be attributed to the neurochemical pathway of circulating sex hormones, it has been suggested that behavior is also influenced by other factors, such as life history and sex-specific gene expression[16]. This indicates a bi-directional relationship between sexual identity and the environment, with far-reaching consequences on cognitive abilities, including learning and memory. How the sexual identity drives molecular and circuit changes towards a shared experience that intersects with learning and survival is still an open question.

The nematode *C. elegans* has been a useful model for the study of learning and memory at the molecular, cellular, neural circuitry, and behavioral levels[17]. Numerous studies have demonstrated that *C. elegans* is capable of non-associative learning and short-term memory, in addition to associative learning, long-term memory, and sensory integration of conflicting cues[18–22].

The two sexes of *C. elegans* display sexually dimorphic behaviors, such as mechanosensory responses to tail touch, dosage-dependent differences in nociceptive behaviors, and chemoattraction to odors and chemicals. Some of these differences have been mapped to corresponding network changes [8,23,24].

Here, we investigated if and how the genetic sex affects the context- and experience-dependent behavioral plasticity when learning a shared environmental cue. We harnessed the well-established model of short-term pathogenic aversive conditioning in *C. elegans* [21,25,26], where

hermaphrodites shift their preference from naïve attraction to aversion upon exposure to the pathogenic bacterium *Pseudomonas aeruginosa* (PA14)[25,27]. We show that males are unable to avoid PA14 as efficiently as hermaphrodites after training. This dimorphic avoidance, however, is not due to differences in the immune responses, but due to layered differences in the sensory and subsequent downstream processing. We observed context-dependent learning when exposing the males to hermaphrodites, which altered their behavior towards PA14. Transcriptomic analyses indicate neuromodulatory regulation, with one candidate, *npr-5*, regulating both the learned as well as context-dependent avoidance by modulating sensory responses. We also unravel the importance of tissue-specific sexual identity and decentralized molecular signaling in regulating male responses. Taken together, our work underscores the diverse levels at which sexual identity modulates dimorphic behavioral responses in each sex towards a shared experience.

Aversive olfactory learning is sexually dimorphic

To test whether short-term aversive learning is sexually dimorphic, we separated virgin males and hermaphrodites and subjected them to an acute training paradigm of pathogenic bacterial exposure (PA14 or *Escherichia coli* strain OP50 as control) that lasted 6 hours, followed by a choice-based test (Fig. 1a). We found that while hermaphrodites efficiently avoided PA14 at the end of the 6-hour mark, males did not display learned aversion (Fig. 1b-c). A similar dimorphic response was observed when we tested the naïve avoidance by exposing either sex to a lawn of PA14 and scored lawn occupancy after 6-8 hours. While males remained within the PA14 lawn, the hermaphrodites' occupancy was minimal (Fig. S1a). We speculated that these observed dimorphisms in short-term learning could arise from differences at checkpoints of information processing within the sexes, such as i) immune responses, ii) integration of sensory information, or iii) a deliberately chosen dimorphic outcome to favor a sex-specific need.

To determine whether the immune system is activated in both sexes to the same extent we imaged the activation of the infection responder gene *irg-1* [28] after 6 hours of exposure to PA14. We found the *irg-1* levels in the anterior gut region of both sexes to be similar (Fig. 1d-e). The similar pathogenic sensitivity was reflected in killing assays conducted to measure PA14 virulence, where both males and hermaphrodites died with similar kinetics (Fig. 1f, Fig. S1b). This is in line with the observation that males do indeed avoid PA14, but only after much more extended training periods (Fig. S1c-d). Thus, even though the immune response of the males was

activated, they were unable to integrate the pathogenicity of PA14 towards learned aversion as rapidly as hermaphrodites.

To evaluate if the avoidance of PA14 is either developmentally timed or inherently dimorphic, we subjected juvenile animals to the same training paradigm as the adult animals (See Methods). We observed that juveniles of both sexes failed to learn and actively preferred PA14 even after training (Fig. S1e-g). This suggests that the dimorphic behavior observed in adulthood is a result of a developmentally mature nervous system[24].

To characterize the impact of sexual identity on the learning axis, we feminized or masculinized specific tissues in hermaphrodites and males, respectively, and subjected them to the learning paradigm (Fig. 1g). When only the nervous system is sex-reversed, hermaphrodites exhibited a dramatic reduction in their learning ability (Fig. 1h-i). Contrary to our expectations, pan-neuronally feminized males failed to learn (Fig. 1j-k), suggesting that the substrate of learned avoidance is restricted mostly to the nervous system in hermaphrodites, but involves additional systems in males. In the absence of a direct link between neuronal regulation and learning in the males, we hypothesized that non-neuronal tissues such as the gut and the germline might affect male learning. Indeed, previous studies have shown the importance of the gut in regulating behavior [29,30]. Yet feminizing the gut of males was also insufficient to enhance learning in males (Fig. 1j-k). Similar results were obtained when analyzing males with a mutated germline, although germline-mutated hermaphrodites seemed to have dampened avoidance (Fig. S1h-i). However, when both the nervous system and the gut were feminized, these males learned to avoid PA14 significantly better than wild-type males (Fig. 1j-k). Thus, the default male drive is orchestrated by several tissues, and their intercommunication is critical for the evaluation and subsequent response to external stimuli.

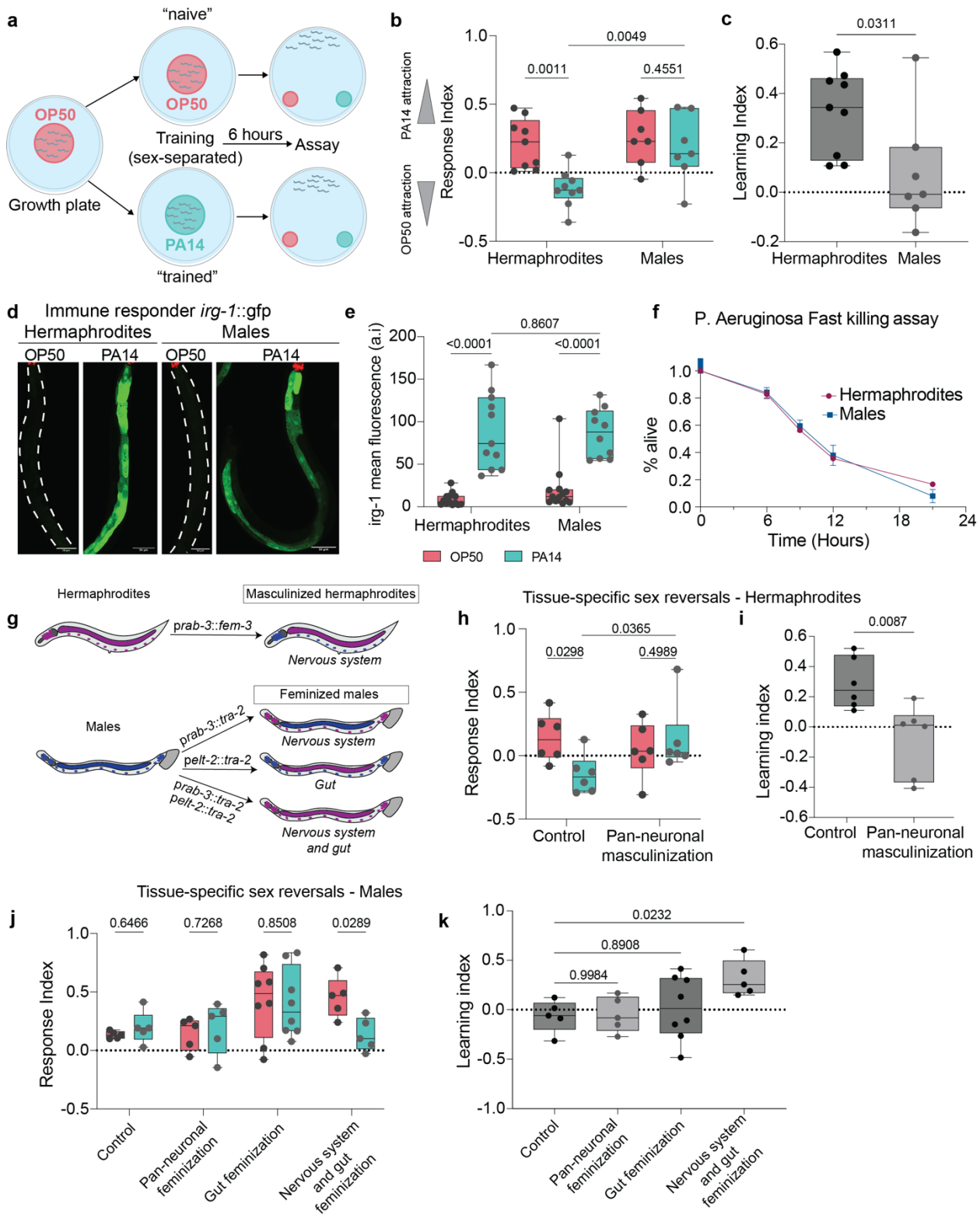

Fig. 1: Distinct tissues govern sexually dimorphic short-term learning of PA14 avoidance

(a) Schematic representation of the training paradigm. A group of *C. elegans* was separated into males or hermaphrodites after late L4, exposed to the pathogenic bacterium *Pseudomonas aeruginosa* (PA14, turquoise, "trained") or OP50 (control, magenta, "naïve") for 6 hours, and then assayed for their response index against OP50 and PA14 (See Methods). **(b)** The Response Index of hermaphrodites [OP50, PA14: *n* = 9] and males [OP50, PA14: *n* = 7] subjected to the training paradigm in A shows dimorphic responses after training. **(c)** The learning indices of hermaphrodites [*n* = 9] and males [*n* = 7] are dimorphic (*n* = biological repeats). **(d)** Confocal micrographs of representative IRG-1::GFP hermaphrodites and males (scale = 50μm) trained on OP50 or PA14 after 6 hours of training. Scale bar at 50μm. **(e)** Quantification of the anterior region of the gut for IRG-1::GFP in hermaphrodites [OP50: N = 13; PA14: N = 11; N = individual animals] and males [OP50: N = 13; PA14: N = 10; N = individual animals] after exposure to OP50 or PA14. **(f)** The percentage of live hermaphrodites [*n* = 3] and males [*n* = 3] in a fast-killing assay, indicating non-dimorphic survival outcomes. **(g)** Schematic representation of the tissue sex-reversal experiments (the results of the equivalent germline experiments are presented in Fig. S1). **(h-i)** Response (H) and Learning (I) Indices of wild-type [OP50, PA14: *n* = 6] and pan-neuronally masculinized (p*rab-3*::*fem-3*) hermaphrodites [OP50, PA14: *n* = 6], showing importance of the nervous system in hermaphroditic learning. **(j-k)** Response (J) and Learning (K) Indices of wild-type (control) males [OP50, PA14: *n* = 5], pan-neuronally feminized (p*rab-3*::*tra-2(ic*)) males [OP50, PA14: *n* = 5], gut-feminized (p*elt-2*::*tra-2(ic*)) males [OP50, PA14: *n* = 5], and pan-neuronally and gut feminized (p*rab-3*::*tra-2(ic*);p*elt-2*::*tra-2*) males [OP50, PA14, *n* = 8], showing inter-tissue regulation of male learning. *n* refers to the number of independent assays with each dot representing a single population assay of 50-200 animals/assay. Box and Whisker plots with mean and entire data range. In (b, e, f, h, j), a two-way ANOVA with Šídák's multiple comparisons test. In (c, i), a Mann Whitney test. In (k), a Brown-Forsythe and Welch's ANOVA with Dunnett's T3 multiple comparisons test. P values are indicated in the figure.

Distinct information processing regulates sexually-dimorphic neuronal signaling

We previously demonstrated that while nociceptive sensory neurons in *C. elegans* respond similarly in the two sexes to a noxious cue (glycerol), the network topology diverges, shaping sexually dimorphic behaviors [8]. The neurons regulating PA14 avoidance have been previously

mapped [31,32]. The sensory neuron AWC is required for odor-mediated attraction, while AWB is required for odor-mediated repulsion [33,34]. In addition, these neurons have been recently established as important in recognizing the odor bouquet presented by PA14 and in regulating both adult and larval learning [31,32,35]. The dimorphic behavior we observed could then arise from distinct computing of environmental cues (i.e., dimorphic neural states lead to dimorphic behavior). To evaluate this, we used calcium imaging to measure the neuronal activity of sensory- and inter-neurons. We observed consistently higher calcium activity upon presentation of PA14 in both the AWB (ON and OFF response) and AWC (OFF response) neurons of naïve males when compared to naïve hermaphrodites (Fig. 2a, c, e-f, Fig. S2a, c, e). The heightened male naïve response provides the first indication of a dimorphic neuronal landscape. After PA14 training, the AWC neuron exhibited a lower response in hermaphrodites (Fig. S2a, e). Despite the lack of learning at the behavioral level (Fig. 1b-c), we nonetheless observed a similar reduction, albeit still higher than trained hermaphrodites, in the response of AWC in males following exposure to PA14 (Fig. S2c, e). The repellent odor-sensitive AWB displayed bi-phasic responses to the PA14 stimulus. We observed no change in the ON response of AWB in either sex, although males consistently showed higher calcium activity (Fig. 2e). However, there was a dimorphic reduction in the OFF response in AWB of trained males when compared to hermaphrodites, indicating that, unlike hermaphrodites, males become less repulsed by PA14 odor after training (Fig. 2a, f). Taken together, these results suggest that behavior is determined by a sensory gating mechanism.

The sensory information from AWC and AWB is passed on to a downstream interneuron AIY, which has been implicated as an information checkpoint that regulates memory retrieval [32,36–38] as well as hermaphrodite training and forgetting states of PA14 aversive learning [26,31]. We observed a reduction in calcium activity after training at the soma of the AIY neuron in both sexes (Fig. S2b, d, f). Yet, within the axonal regions of AIY, we observed a decrease in calcium activity after training only in hermaphrodites (Fig. 2b, g) but not in males (Fig. 2d, g). To determine whether the observed dimorphisms in neuronal activity also extend to the synaptic output of AIY, i.e., a readout of the learning process, we used a fluorescent readout of RAB-3, which regulates synaptic vesicles [39]. The axonal regions of AIY can be distinguished according to their respective synaptic partners as Zone 2 and 3 [39]. We quantified the mCherry expression levels of RAB-3 (Fig. 2h) after training with PA14 and observed a non-dimorphic decrease in

RAB-3 levels in both Zones 2 and 3 (Fig. 2i, Fig. S2g), suggesting that the sensory stimulus is processed in both sexes. However, we noticed that the extent of difference in RAB-3 expression between the naïve and trained males is lower than that of hermaphrodites (Fig. 2j). Thus, AIY soma and axonal responses indicate a compartmentalized sexual dimorphism in neuronal signaling. Taken together, our results show an increased sensory response to PA14 in AWB, and a subsequent decrease in the AIY interneuron only in hermaphrodites, suggesting that dimorphic perceptive information is being communicated downstream.

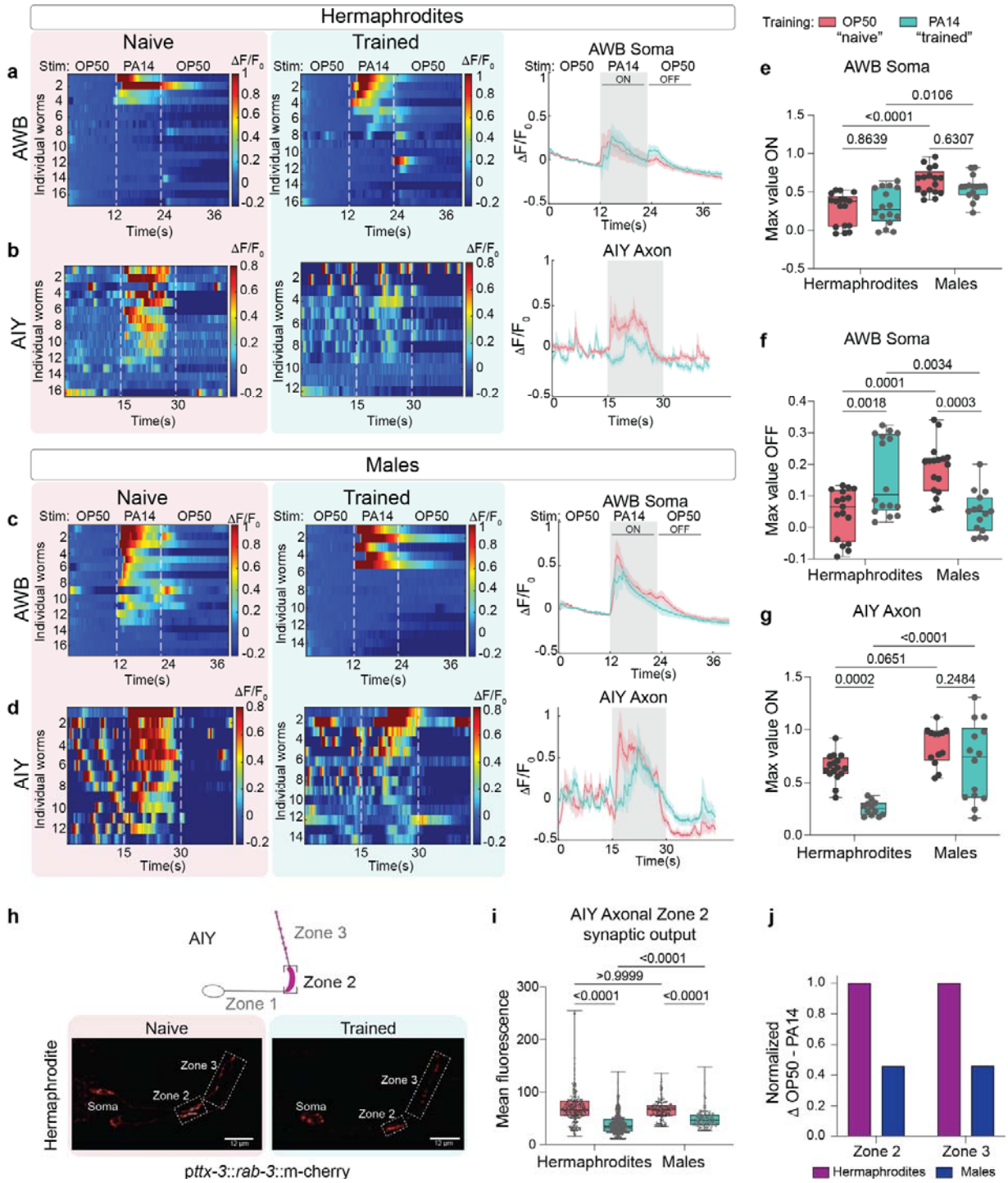

Figure 2: Distinct dimorphic compartmentalized information processing in response to PA14 stimulus. (a-b) From left to right, heatmap of GCaMP signals of select neurons in naïve (magenta) and trained (turquoise) hermaphrodites and the SEM traces of both naïve and trained animals. The shaded region in the SEM traces corresponds to the exposure window of PA14 supernatant on both naïve and trained animals. OP50 supernatant was used as the buffer. (See

Methods) (a) AWB calcium levels in trained hermaphrodites [N = 16] rise in response to PA14 supernatant compared to naïve animals [N = 17]. (b) AIY axonal calcium levels in trained hermaphrodites [N = 12] decline in response to PA14 supernatant compared to naïve animals [N = 16]. **(c-d)** From left to right, heatmap of GCaMP signals of select neurons in naïve (magenta) and trained (turquoise) males and the SEM traces of both naïve and trained animals. The shaded region in the SEM traces corresponds to the exposure window of PA14 supernatant on both naïve and trained animals. OP50 supernatant was used as the buffer. (See Methods) (c) AWB calcium levels in trained males [N = 15] decline in response to PA14 supernatant compared to OP50 [N = 17] supernatant. (d) AIY axonal calcium levels in trained males [N = 14] show no decrease in response to PA14 supernatant compared to naïve animals [N = 13]. **(e-g)** Moving mean quantification of AWB ON (e), AWB OFF (f) and AIY axon (g) in naïve (magenta) and trained (turquoise) hermaphrodites and males. AWB soma (e-f) shows dimorphic OFF activation states, namely hermaphrodites increase activation after training while males show reduction. AIY axon (g) shows dimorphic values with hermaphrodites showing a reduction after training and males show no significant change. **(h)** Representative heatmap confocal micrographs of p*ttx-3*::*rab-3*::m-Cherry in naïve and trained hermaphrodites showing expression in distinct zones of AIY namely, a synapse-devoid Zone 1 and synapse-rich Zones 2 and 3. Scale bar at 12µm. **(i)** Synaptic RAB3 mCherry fluorescence in AIY Zone 2 axonal regions shows a non-dimorphic reduction in synaptic output but a dimorphic degree of change between the sexes upon training. Each dot represents a puncta from 13-36 animals per group. **(j)** Normalized delta between naïve and trained RAB-3 expression of both sexes in Zone 2 and Zone 3. Hermaphrodites in magenta and Males in blue. Data is normalized to hermaphrodites. Box and Whisker plots with mean and entire data range. In (a-g), n refers to number of animals of each group. In (e-g), a two-way ANOVA with Tukey's multiple comparisons test. In (i), a Kruskal-Wallis test with Dunn's multiple comparisons test. Box and Whisker plots with mean and entire data range. P values are indicated in the figure.

Dimorphic transcriptional landscape of naïve and trained animals

To characterize the molecular landscape of short-term dimorphic learning, we performed whole-animal transcriptomics on naïve and trained hermaphrodites and males using a modified version of the MAR-seq protocol[40]. To visualize the relationship between training and sexual identity

across all experimental groups, we performed a principal component analysis (PCA) on the ~ 12,000 identified genes. The PCA revealed a clear separation by the sex and training status of the animals (Fig. 3a-b). This finding was further validated by the dimorphic expression of *tra-2* (higher in hermaphrodites[41]) and *pkd-2* (higher in males[42]) (Fig. S3a). We found 869 and 846 differentially expressed genes in hermaphrodites and males, respectively, after training (FDR < 0.05; data S4). Unlike the behavioral results, where both naïve and trained males displayed similar attraction towards PA14 (Fig. 1b-c), their molecular landscape reflects the training experience (Fig. 3b). Volcano plots and functional GO term analysis revealed similar changes in immune regulation, fatty acid metabolism, and other stress-related pathways in both sexes, an expected outcome given the gustatory and pathogenic nature of the training bacterium (Fig. 3c-d, Fig. S3b). This is also reflected in the majority of genes shared between the sexes after training (Fig. S3c). However, differences begin to emerge when looking at each sex separately (Fig. S3d). Of the entire transcriptomics dataset, 70 genes were previously reported to be involved in PA14-related behaviors [26,27,30,32,43–54]. Consistent with our survival assays, most of the genes implicated in PA14 survival, such as *daf-16* and *daf-7*, were non-dimorphic. Interestingly, the levels of *ins-11* [51], a negative regulator of PA14 avoidance, and genes involved in training and forgetting, such as *gst-38 and gst-26* [26], were similarly regulated in trained animals of both sexes (Fig. S3e). These results suggest that an underlying modulatory mechanism might regulate the observed male behavior.

Sexually dimorphic modulation of the NPY receptor *npr-5* expression

To identify transient changes in the learning process specific to each sex, we focused on differentially expressed neuro-specific gene classes such as receptors and neuropeptide families (Fig. 3e). Neuropeptide receptor *npr-5*, which is involved in regulating foraging and fatty acid metabolism in hermaphrodites [55,56], emerged as a likely candidate, as it was down-regulated in males after training (Fig. 3e). Notably, NPR-5 is an ortholog of the mammalian NPY receptor, a key regulator of various behaviors, including learning and memory [57–61]. In order to determine its change in expression post-training, we endogenously tagged *npr-5* using CRISPR-cas9 gene-editing and quantified its expression levels in head sensory neurons, previously described to regulate behavior [55,56] (Fig. 3f). Consistent with previous studies [55], NPR-5 was observed in body wall muscles and multiple neurons, including sensory neurons (Fig. 3f). After training, NPR-5 levels rose in hermaphrodite AWB neurons but were reduced in male AWB neurons (Fig. 3g).

Intriguingly, this change in NPR-5 expression resembles the activity levels of AWB (Fig. 2f). Although ASJ has been previously described to be involved in processing PA14 experience[30,54,62], and AIY displayed dimorphic response (Fig 2b, d, g), no significant changes were observed in NPR-5 expression after training in ASJ and AIY (Fig. 3g). These results support the transcriptomic data, suggesting NPR-5 is down-regulated in males upon PA14 exposure (Fig. 3e), pointing to a critical role of *npr-5* in modulating learning, perhaps at the sensory level.

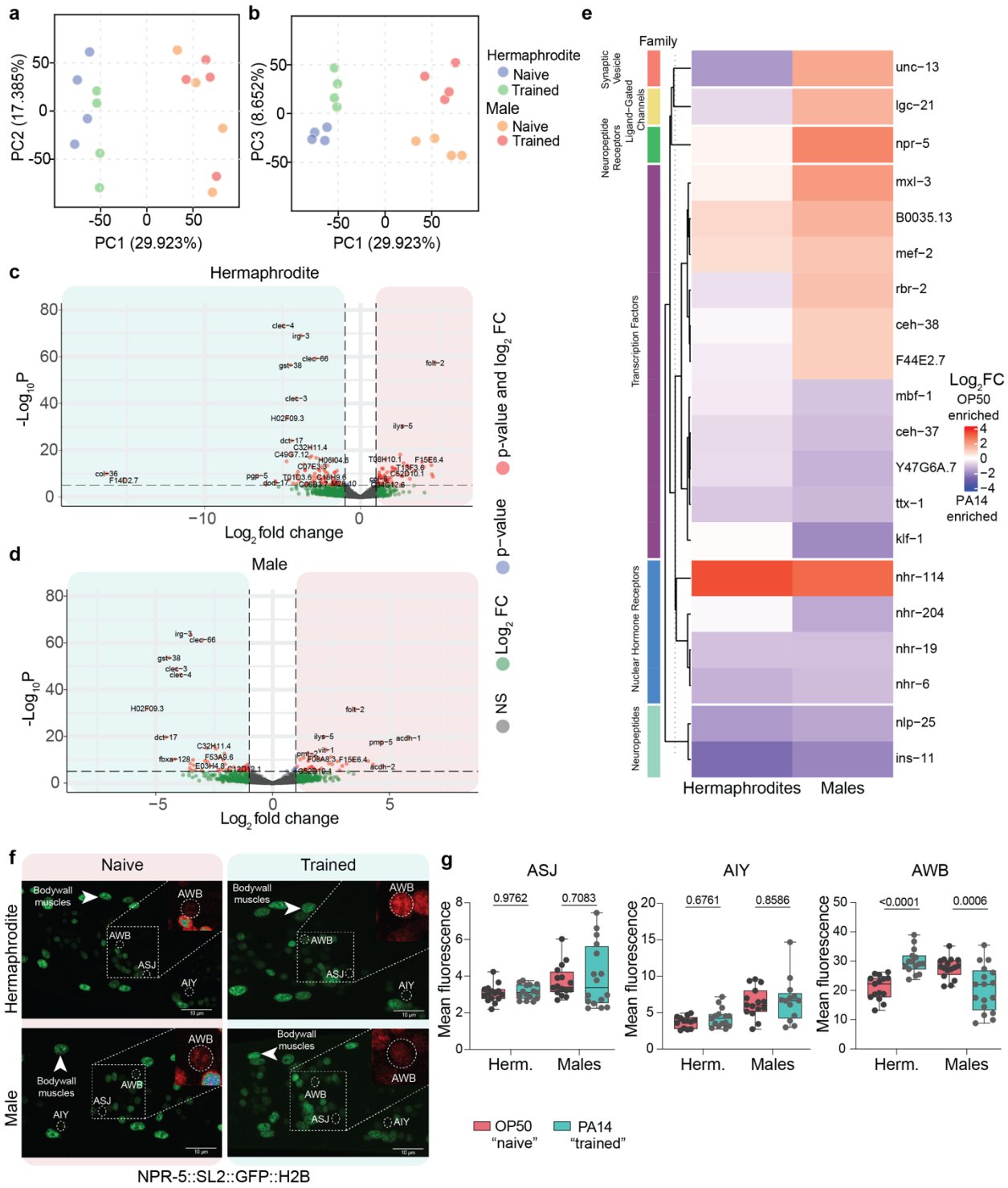

Figure 3: Sexually dimorphic learning triggers sex-specific NPY expression. (a-b) Principle Component Analysis (PCA) of the transcriptomes of hermaphrodites and males (n = 4 independent samples from 600-800 animals/replicate) after training, ordered according to sex (a) and training status (b), showing the validity of the data in separating the sexes and training states

by transcriptomics. **(c-d)** Volcano plots of naïve and trained hermaphrodites (c) and males (d), depicting similar changes in transcripts **(e)** Heatmap of $\log_2$ foldchange of neuron-relevant genes from naïve vs. trained males (FDR < 0.05) and hermaphrodites. Red indicates enrichment in naïve animals (OP50), while blue indicates enrichment in trained animals (PA14). **(f)** Representative confocal micrographs of NPR-5::SL2::GFP CRISPR knock-in in naïve and trained hermaphrodites and males showing expression in body wall muscles and sensory cells. Inset shows heatmap expression of NPR-5 GFP in the selected region with AWB and ASJ. Scale bar at 10µm. **(g)** Quantification of mean fluorescent signals of NPR-5 in ASJ, AIY and AWB, showing dimorphic expression changes in AWB after training [ASJ [hermaphrodites: OP50, PA14 N =15; males: OP50, PA14 N =16]; AIY [hermaphrodites: OP50 N =13, PA14 N =15; males: OP50 N =15, PA14 N =13]; AWB [hermaphrodites: OP50, PA14 N =15; males: OP50 N =16, PA14 N =17]. N refers to the number of individual animals in each group. In (g), two-way ANOVA with Šídák's multiple comparisons test. Box and Whisker plots with mean and entire data range. P values are indicated in the figure.

Neuropeptidergic modulation of state- and sex-specific learning

To evaluate the extent of neuropeptidergic regulation in male-specific PA14 aversive learning, we subjected *npr-5* mutants to the training paradigm. Strikingly, males with a partial or full *npr-5* deletion acquired the ability to learn quickly in a similar fashion as wild-type hermaphrodites (Fig. 4a-d). Although mutant *npr-5* hermaphrodites still avoided PA14, no significant changes were observed between the naïve and trained responses (Fig. 4a, c). Since our observed expression of *npr-5* (Fig. 3f-g) and previous studies [55] indicate a sensory-specific site-of-action of *npr-5*, we rescued *npr-5* expression in ciliated neurons, including AWB, in *npr-5* mutant background. This sufficed to impede the learning ability, reverting the animal back to the wild-type male phenotype (Fig. 4a-b). Thus, *npr-5* is required for suppressing learned avoidance, and its activity suggests a possible sensory gating mechanism in males, in line with the observations made in the neuronal activity of trained males (Fig. 2).

Previous studies have established the link between various neuropeptides and regulation of behavioral states[62,63]. Given the dimorphic neuropeptidergic landscape (Fig. 3d) and the decentralized learning processing we observed in males (Fig. 1j-k), we postulated that the learning behavior in males might be regulated by multiple signaling molecules in a molecular

network (Fig. 4e). Indeed, when we screened select candidate neuropeptides using mutants or RNAi, we observed that several neuropeptides such as *flp-33*, *flp-3* and *flp-18*, a cognate ligand of *npr-5*, were involved (Fig. 4f-h). The complex regulation of male PA14 aversive learning by *npr-5* and multiple neuropeptides demonstrates that male learning is an amalgamation of complex internal processing.

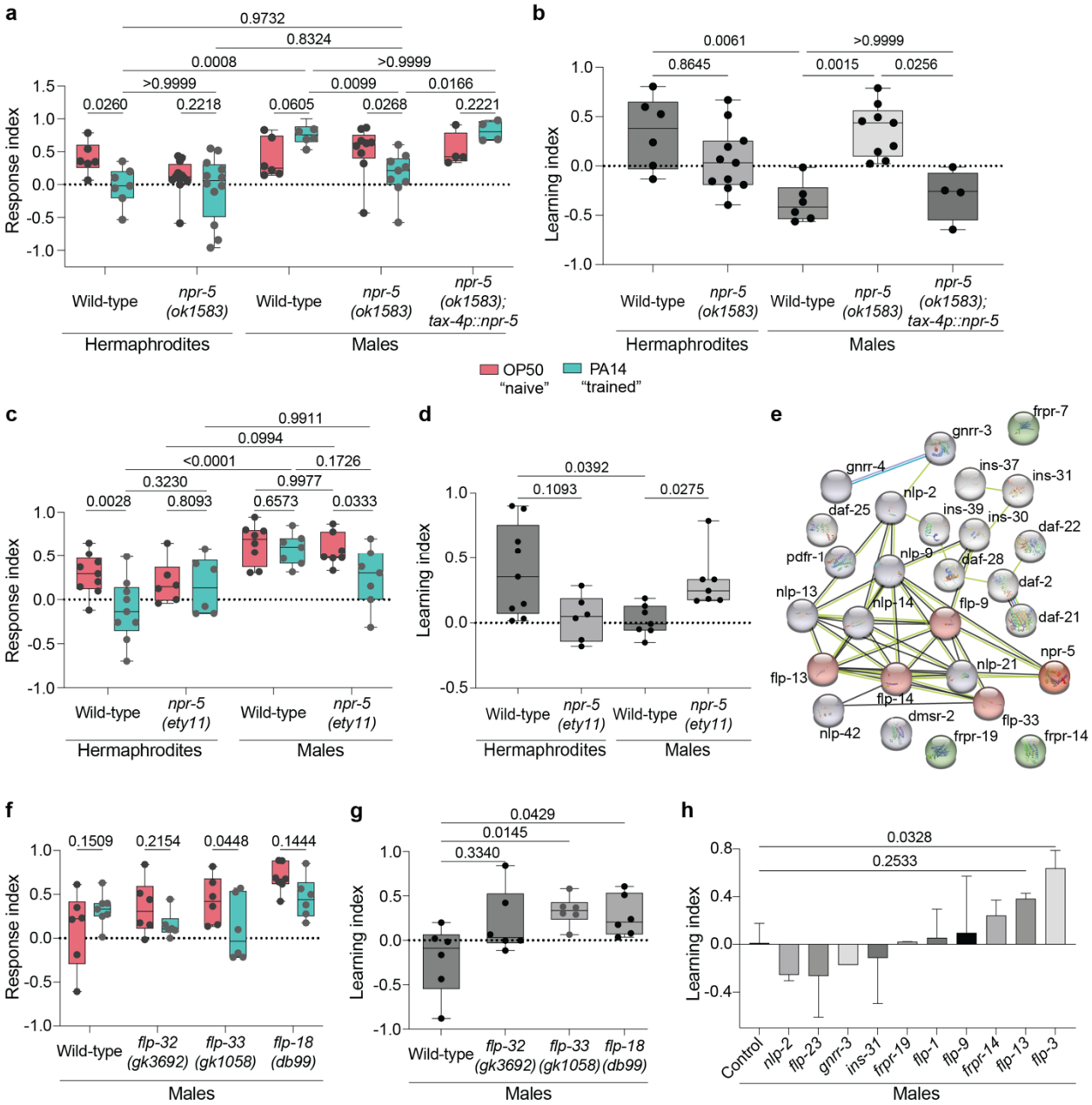

Figure 4: NPR-5 regulates male-specific behavior. (a-b) Response (a) and Learning (b) Indices of naïve (magenta in (a)) and trained (turquoise in (a)) wild-type and *npr-5* mutant hermaphrodites and males and a male rescue strain where *npr-5* cDNA was expressed under a

tax-4 promoter; data shows sex-specific behavioral effects in males [Response Index: wild-type hermaphrodites: OP50 *n* = 6, PA14 *n* = 7; *npr-5* hermaphrodites: OP50, PA14 n = 12; wild-type males: OP50, PA14 n = 6; *npr-5* males: OP50, PA14 n = 9; p*tax-4*::*npr-5*cDNA;*npr-5* males: OP50, PA14 n = 4. Learning Index: wild-type hermaphrodites: *n*=6; *npr-5* hermaphrodites: *n* = 12; wild-type males: *n* = 6; *npr-5* males: *n* = 9; p*tax-4*::*npr-5*cDNA;*npr-5* males: *n* = 4]. **(c-d)** Response (c) and Learning (d) Indices of naive (magenta in (c)) and trained (turquoise in (c)) wild-type and *npr-5* CRISPR mutant hermaphrodites and males, showing sex-specific behavioral effects in males [hermaphrodites: OP50, PA14, Learning Index *n* = 9; *npr-5* hermaphrodites: OP50, PA14, Learning Index *n* = 6; males: OP50, PA14, *n* = 8, Learning index *n* = 7; *npr-5* males: OP50, PA14, Learning Index *n* = 7]. **(e)** Schematic of all the neuropeptide-related genes from our dataset using String Protein Ensemble[64] showing interactions between several candidate genes, including *npr-5*. **(f-g)** Response (f) and Learning (g) Indices of wild-type [OP50 *n* = 6, PA14 *n* = 7, Learning Index *n* = 6], *flp-32* (*gk3692*) mutant [OP50, PA14, learning index *n* = 6], *flp-33* (*gk1058*) mutant [OP50, PA14, Learning Index *n* = 6] and *flp-18* (*db99*) mutant males [OP50, *n* = 7, PA14, Learning Index *n* = 6], showing peptidergic regulation of male learning. **(h)** Learning Indices of RNAi-treated males showing *flp-3* as a likely neuromodulator [control: *n* = 5; *gnrr-3*: *n* = 1; *nlp-2*, *flp-23*, *ins-31*, *frpr-19*, *flp-1*, *flp-9*, *frpr-14*, *flp-13*, *flp-3*: *n* = 2]. In (a, c), a two-way ANOVA with Šídák's multiple comparisons test. In (b, d, g, h), a Kruskal-Wallis test with Dunn's multiple comparisons test. In (f), a two-way ANOVA with Tukey's multiple comparisons test. *P* values are indicated in the figure.

npr-5 functions in AWB to modulate PA14 responses

Based on its sensory responses to PA14 (Fig. 2a, c, e-f), the observed decrease in *npr-5* expression following training (Fig. 3g), and the change in behavior upon rescue (Fig. 4a), AWB is a likely site of action for *npr-5*. We, therefore, measured AWB activity in *npr-5* mutants and observed a striking change in firing pattern, namely, a heightened OFF response (Fig. 4a, c), compared to wild-type animals (Fig. 2a, c). In addition, only *npr-5* mutant male AWB neurons exhibited a stronger response to the removal of the PA14 stimulus after training (Fig. 4c,e), similar to wild-type hermaphrodites (Fig. 2a, c, e-f). This further strengthens the notion that *npr-5* acts in AWB to inhibit the proper integration of PA14 signals.

Even though we observe no change in *npr-5* expression in AIY (Fig. 3g), there is a stark decline in the AIY soma calcium activity in only naïve, but not trained, *npr-5* mutants (Fig. S4a-c) compared to wild-type animals (Fig. S2b, d), suggesting that *npr-5* is involved in the recognition and processing of PA14 in the naïve state. Similar observations were made in the axonal responses of AIY to PA14 odor in naïve mutant hermaphrodites and males (Fig. 5b, d, f). In contrast to wild-type males, which retained high activation after training (Fig. 2d, g), mutant males showed reduced activation (Fig. 5b, d, f). Taken together, these results suggest that *npr-5* plays a crucial role in the integration of PA14 naïve cues in both sexes, but also the trained responses of males. This is highlighted also at the synaptic level where the RAB-3 expression of *npr-5* mutant males displays an increase in mean fluorescence after training (Fig. 5g), unlike wild-type animals (Fig. 2i) and *npr-5* mutant hermaphrodites (Fig. 5g). Thus, exposure to PA14 is processed dimorphically between the sexes, altered partly through modulation by *npr-5* in males.

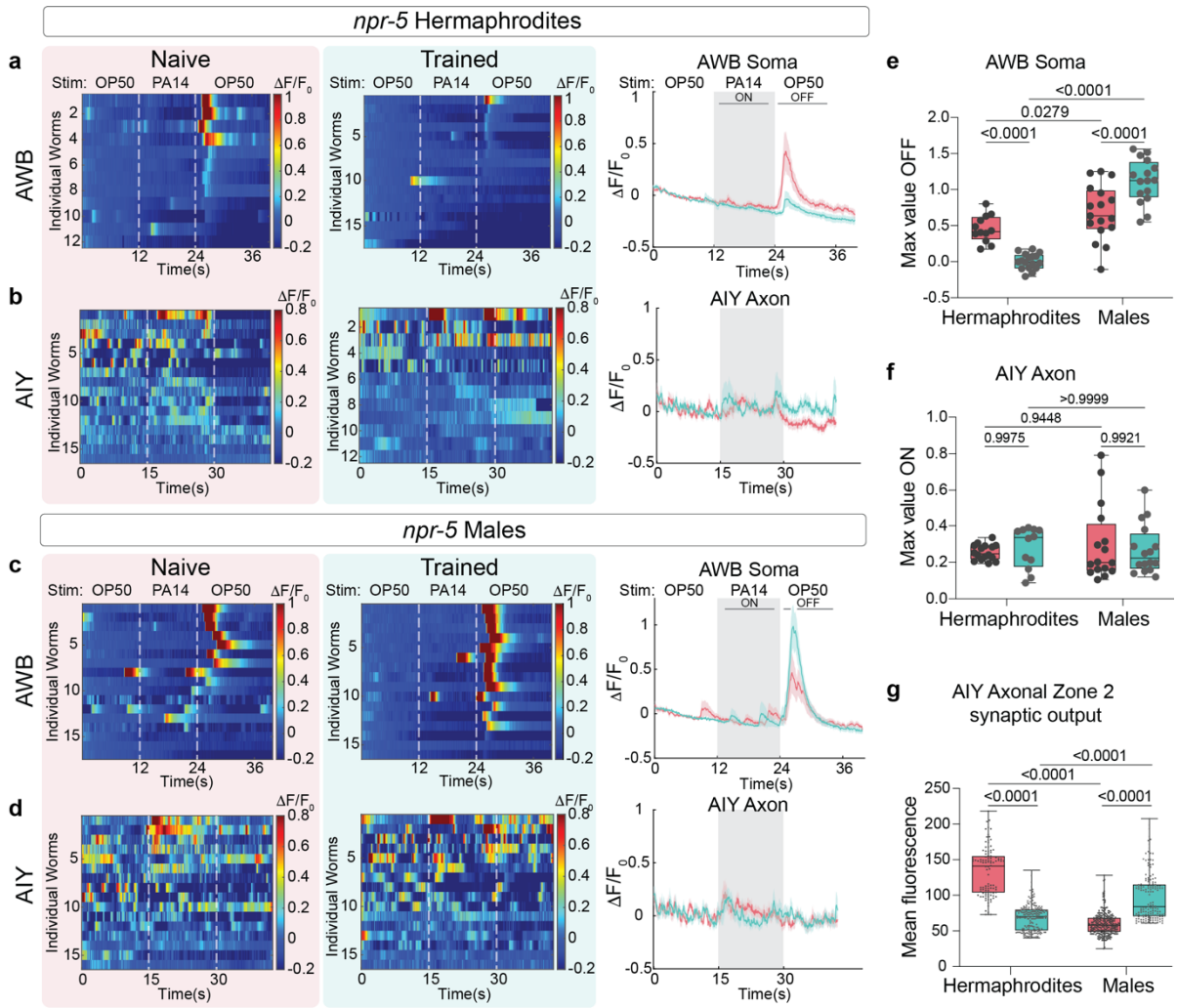

Figure 5: NPR-5 modulates state and sex-specific neuronal activity. (a-b) From left to right, heatmap of GCaMP signals of AWB and AIY neurons in naïve (magenta) and trained (turquoise) *npr-5* hermaphrodites and the SEM traces of both naïve and trained animals. The shaded region in the SEM traces corresponds to the exposure window of PA14 supernatant on both naïve and trained animals. OP50 supernatant was used as the buffer. (See Methods). (a) AWB soma calcium response of naïve and trained *npr-5* mutant hermaphrodites to PA14 supernatant [OP50 N = 12, PA14 N = 16] exhibiting a reduction in the calcium response after the PA14 stimulus. (b) AIY axonal calcium levels in both naïve and trained *npr-5* hermaphrodites [N = 16] decline in response to PA14 supernatant compared to naïve animals [N = 12]. **(c-d)** From left to right, heatmap of GCaMP signals of AWB and AIY neurons in naïve (magenta) and trained (turquoise) *npr-5* males animals and the SEM traces of both naïve and trained animals. The shaded region in the SEM traces corresponds to the exposure window of PA14 supernatant on both naïve and

trained animals. OP50 supernatant was used as the buffer. (See Methods). (c) AWB soma calcium response of naïve and trained *npr-5* mutant males to PA14 supernatant [OP50 N = 17, PA14 N = 16] exhibiting an increase in the calcium response after the PA14 stimulus. (d) AIY axonal calcium levels in both naïve and trained *npr-5* males [N = 16] decline in response to PA14 supernatant compared to naïve animals [N = 16]. **(e-f)** Moving mean quantification of AWB OFF (e) and AIY axon ON (f) in naïve (magenta) and trained (turquoise) hermaphrodites and males. AWB soma (e) shows dimorphic OFF activation states, namely hermaphrodites decrease activation after training while males show an increase. AIY axon (f) shows non-dimorphic values with both *npr-5* hermaphrodites and males showing no significant change. **(g)** Mean quantification of synaptic RAB3 mCherry fluorescence in naïve and trained *npr-5* mutant hermaphrodite and male AIY shows dimorphic responses, marked by a decrease in hermaphrodites and an increase in males upon PA14 training. In (a-f) N refers to the number of individual animals of each group, in (g), each dot represents a puncta from 10-17 animals per group. Box and Whisker plots with mean and entire data range. In (e, f), a two-way ANOVA with Šídák's multiple comparisons test. In (g), a Two-way ANOVA with Tukey's multiple comparisons test. *P* values are indicated in the figure.

NPR-5 overexpression curbs sexual-conditioning-mediated learning

Our pathogen-sensitivity and calcium-imaging results suggest that while males possess the ability to recognize and potentially process the PA14 experience (Fig. 1c-d, S2), learning is repressed. As *C. elegans* males will abandon food in search of mates [24], we hypothesized that perhaps repression is a result of inherent evolutionary drives. Therefore, diminishing males' sexual drive could lead to PA14 avoidance. To assess this, we trained animals with the other sex ("sex-exposed") or without ("virgin") in the presence of either OP50 (Fig. 6a) or PA14 (Fig. 6b) and checked their response indices. Sexual conditioning would predict that in the presence of hermaphrodites, the males would be highly attracted to the coupled stimulus, as evidenced by the retention of attraction to OP50 by the naïve hermaphrodite-exposed males (Fig. 6b). Surprisingly, we observed that, as opposed to virgin-trained males, which retain their attraction to PA14, trained hermaphrodite-exposed males show decreased attraction to PA14 (Fig. 6d). Our results suggest that reducing the males' sexual or mate-searching drive might allow the trained decision-making process to flow uninterrupted. To assess the potential role of *npr-5* in regulating

the integration of the internal state into the learning circuit, we overexpressed *npr-5* in sensory neurons of wild-type males to simulate a perpetual 'naïve' state (Fig. 6b). These males failed to avoid PA14, even after training, regardless of their sexual status (Fig. 6d). Taken together, these results suggest that sex-specific needs act as a regulator of male learning, dictated and processed by the inherent neuromodulatory state, where *npr-5* in the sensory neurons of males acts as a sensory 'door-stopper' that halts any potential learning by modulating the diverse variables that impinge on male decision-making (Fig. 6e).

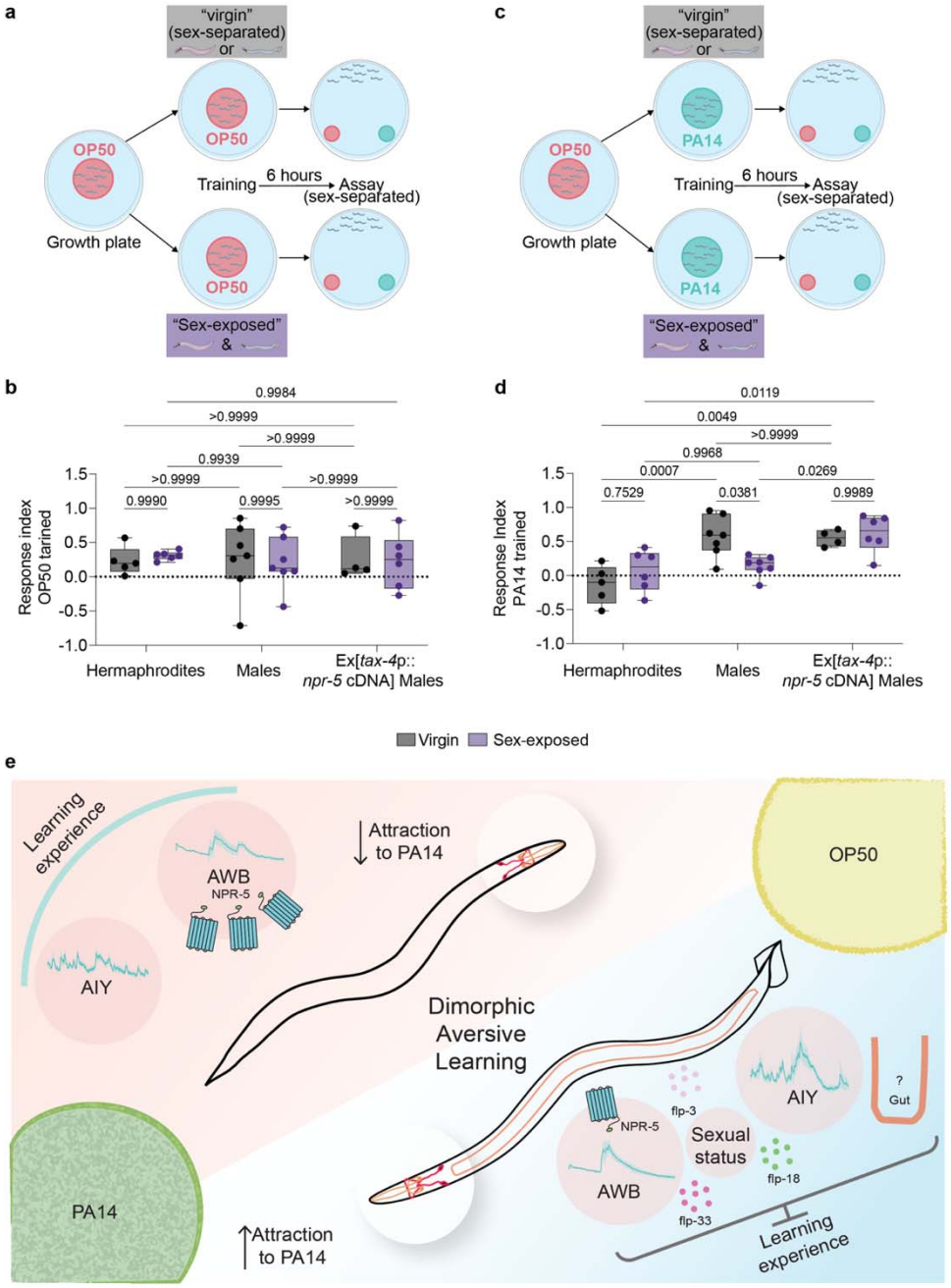

Figure 6: Sexual status determines behavioral outcome. (a) Schematic representation of the conditioning training paradigm. A group of *C. elegans* was separated into males or hermaphrodites after late L4, exposed to the benign bacterium OP50 (magenta) for 6 hours either separately ("virgin") or both sexes together ("sex-exposed"), and then assayed for their response index against OP50 and PA14 (See Methods). **(b)** Response Index of OP50-exposed virgin and sex-exposed wild-type hermaphrodites [virgin n = 5, mated n = 6], wild-type males [virgin,

mated *n* = 7] and *npr-5*-overexpression mutant (p*tax-4*::*npr-5*cDNA) males [virgin *n* = 4, mated *n* = 6], showing no neuromodulatory regulation of sexual-conditioning-mediated changes in naïve males. **(c)** Schematic representation of the training paradigm. A group of *C. elegans* was separated into males or hermaphrodites after late L4, exposed to the pathogenic bacterium *Pseudomonas aeruginosa* (PA14, turquoise) for 6 hours either separately ("virgin") or both sexes together ("sex-exposed"), and then assayed for their response index against OP50 and PA14 (See Methods). **(d)** Response Index of PA14-exposed virgin and sex-exposed wild-type hermaphrodites [virgin *n* = 5, mated *n* = 5], wild-type males [virgin *n* = 7, mated *n* = 7] and npr-5-overexpression males [p*tax-4*::*npr-5*cDNA virgin *n* = 4, mated *n* = 6] showing neuromodulatory regulation of sexual-conditioning-mediated avoidance in males. **(e)** Schematic of sexually dimorphic response to PA14. A short-term exposure causes hermaphrodites to avoid PA14, while generating neuronal representations in AWB as a higher OFF response and a reduced response in AIY axonal regions. In males however, PA14 exposure generates a dimorphic neuronal representation. AWB shows no OFF response and AIY shows no reduction. The avoidance is then modulated by *npr-5, flp-3, flp-33, flp-18* and the sexual status. There are indications of additional regulators, possibly from the gut. All of these mechanisms together, drive the repressed learning and continued choosing of PA14 by the males. *n* refers to number of independent assays with each dot representing a single population assay of 50-200 animals/assay. In (b, d), a Two-way ANOVA with Tukey's multiple comparisons test. *P* values are indicated in the figure.

Discussion

Sex-specific behaviors have long been recognized as both products and drivers of sexual selection, however learning, a sex-shared trait, would naïvely be expected to withstand the forces of sexual selection, as it is crucial to an organism's survival. Notably, a recent study demonstrated that in a limited information paradigm, female rats outperform males[65]. These findings underscore the importance of evaluating learning within the context of survival, where information is rapid, limited, and temporal. In our study, we investigated the learning performance of both *C. elegans* sexes in a multi-factorial, ethologically relevant paradigm, specifically focusing on pathogen avoidance. Our results reveal an intriguing behavioral

dimorphism: Males do not learn to avoid the pathogenic bacteria PA14 as efficiently and rapidly as hermaphrodites.

The exposure to PA14 generates a neural representation of that experience[26,31,32]. Indeed, we observe that two major olfactory neurons AWC and AWB and a cholinergic interneuron AIY reflect that training experience. Consistent with our notion that males are able to process the training experience, we observe that the somas of both AWC and AIY reduce their responses to PA14 supernatant, in a manner similar to that of hermaphrodites. However, males exhibit a distinct neural representation after training. The OFF responses of AWB were sexually dimorphic; it increased in hermaphrodites but reduced in males. Parallelly, the axonal regions of male AIY remain unaffected but that of hermaphrodites showed a reduction analogous with their AIY somas. Although compartmentalization of information processing has been shown before [66], we uncover a possible sexually dimorphic component. The neuropeptide receptor *npr-5*, maintains these neural states as its mutation caused a switch in male AWB OFF responses, which heightened after training, and a complete silencing of naïve AIY responses. These point to the existence of a sensory gating mechanism in the males where information is diverted, partly through *npr-5*, so as to continue choosing PA14 over OP50 until the repression is alleviated.

Thus, in our investigation of the underlying molecular mechanisms that drive these behavioral disparities, we identified several notable divergences in how males and hermaphrodites process shared information during the learning process (Fig. 5e). First, learning in hermaphrodites appears to be contingent on their nervous system, whereas males require the combined processing of both their nervous system and gut to make critical choices between benign and pathogenic bacteria. This indicates the existence of a complex regulatory mechanism in males that overrides the immediate threat of infection, a finding in line with recent evidence highlighting the importance of the gut-brain axis in behavior regulation [30,67]. Our study further suggests the presence of a sexually dimorphic component. A potential explanation is the dispersed network of neuropeptides we uncovered that could partially function from the gut. Second, our investigation of neuronal correlates of learning revealed distinct sex-specific activation levels and responses to PA14 stimuli in the sensory neurons and interneurons examined. This observation adds another facet to the developing proposal of the sex differences in synaptic mechanisms that underlie plasticity, learning, and memory [7]. Sex hormones have been shown to play a role in learning [68,69]. Importantly, our study highlights the role genetic sex

plays in neuronal function independent of sex hormones. Lastly, the MAR-seq analysis of naïve and trained animals points to transcriptomic differences between males and hermaphrodites, particularly within the underlying neuromodulatory network that potentially contributes to the observed behavioral differences. Similar findings have been reported in butterflies, where a genomic analysis revealed a tissue and gene family-specific bias between the sexes that could explain learning dimorphisms [70]. Recent evidence highlights the important role of neuromodulators in recognizing and avoiding PA14 [44,48]. Consistent with this, we demonstrate that the sensory modulation of NPR-5 expression is not only crucial for male behavior but also for the maintenance of neuronal firing patterns.

A key question arises regarding the potential influence of evolutionary pressures. Our data suggest that while males do eventually learn to avoid PA14, they might exhibit short-term repression as a behavioral adaptation. Drawing a parallel to models of foraging animals that exhibit overharvesting or over-staying [71], it may be evolutionarily beneficial for *C. elegans* males to stay in a patch of pathogenic bacterium, despite immunological activation, to maximize the chances of encountering incoming hermaphrodites. Supporting this notion is the observed reduction in attraction towards PA14 in mated males. One interpretation of this finding is that by removing the need to search for mates, the mating pressure is reduced in males, thus allowing them to activate the otherwise gated behavior. This observation is further supported by recent evidence of increased mating by hermaphrodites previously exposed to pathogenic bacterium[72]. It is tempting to speculate that these two pathways co-evolve to maximize organismal fitness under dire conditions. In such a scenario, the overall evolutionary demand of the species is fulfilled, albeit in a complex sex-specific manner. A fascinating example is the lower participation of the male bumblebee in cognitive tasks [73], even though they share comparable learning abilities with sterile worker females [74], suggesting that nuanced sex-specific roles alter the perceived learning objective for each sex. Therefore, considering the sex differences in decision-making behavior across organisms, it stands to reason that sexual selection impinges on learning behaviors to favor sex-specific outcomes. By assessing the influence of sexual identity at key levels involved in learning, such as molecular and neuronal circuits, we emphasize the importance of considering sex differences in learning and memory disorders.

Acknowledgments: We thank the members of Oren-Suissa lab for their insights regarding the manuscript. We especially thank Dr. Yehuda Salzberg who helped us in generating the npr-5 CRISPR strain used in this study. We would like to thank Mario De Bono for furnishing us with much-needed strains. Some strains were provided by the CGC, which is funded by the NIH Office of Research Infrastructure Programs (P40 OD010440). We would also like to thank Prof. Sivan Korenblit for plasmids. We would like to extend our gratitude to the Nano-Fabrication unit and the Genomics Sandbox unit at the Life Science Core Facility of Weizmann Institute of Science for helping us with the PDMS chips and the transcriptomics, respectively. We thank WormBase, the online database of *C. elegans* genes, for the excellent curation of various information regarding each gene.

Methods

Strains and experimental design

The *Caenorhabditis elegans* strains included in the study are as follows: *him-5*(e1490)(Figs. 1-6 and Figs. S1-S4), MOS515 *agIs17*[*Pmyo-2::mCherry::irg-1p::GFP+him-5(e1490)*](Fig. 1), UR236 *fsIs15*[*Prab-3::fem-3(+)::SL2::mCherry::Punc-122::GFP+him-5(e1490)*](Fig. 1), OH14507 *otEx6775*[*Prab-3::tra-2(ic)::SL2::NLS::tagRFP+otIs525*(*lim-6(intron4)::gfp*)+ *him-5(e1490)*] (Fig. 1), MOS309 *etyEx80*[*elt-2::tra-2::Tag-RFP 10 ng/ul + ttx-3::mCherry 20 ng/ul + PBS 70 ng/ul + him-5(e1490)*](Fig. 1), MOS517 *otEx6775*[*Prab-3::tra-2(ic)::SL2::NLS::tagRFP); etyEx80[elt-2::tra-2::Tag-RFP 10 ng/ul + ttx-3::mCherry 20 ng/ul + PBS 70 ng/ul]+ him-5(e1490)*](Fig. 1), MOS373 [*glp-1(e2141) + him-5(e1490)*](Fig. S1) , MOS574 *kyEx4275*[*str-2::GCaMP5A::unc-122::dsRed) + him-5(e1490)*](Fig 2), MOS645 *syEx*[*str-1::GCaMP3;str-1p::dsred; pha-1rescue]+(pha-1; lite-1) + him-5(e1490)*](Fig. 2), MOS301 *kyEx4857*[*mod-1::GCaMP5::myo3::cherry + him-5(e1490)*](Fig. 2 and Fig. S2), MOS165 *olaEx1316*[*Pttx3::CD4::GFP(11)+Pglr-3::CD4::GFP(1-10) + Pttx-3::mCherry::rab-3 + unc-122p::GFP + him-5(e1490)*](Fig. 2 and Fig. S2), MOS618 [*syb5786(npr-5::GFP CRISPR) + etyEx230 (ttx-3::mCherry) + him-5(e1490)*](Fig. 3), MOS438 [*npr-5(ok1583) + him-8(e1489)*](Fig. 4), MOS559 [*npr-5(ety11) + him-5(e1490)*](Fig. 4), MOS753 [*npr-5(ok1583)+ Ex(Ptax-4::npr-5 cDNA; unc-122:GFP)+him-5(e1490)*](Fig. 4), MOS613 [*flp-32(gk3692[loxP + myo-2p::GFP::unc-54 3' UTR + rps-27p::neoR::unc-54 3' UTR + loxP]) + him-5(e1490)*](Fig. 4), MOS612 [*flp-33(gk1038) + him-5(e1490)*](Fig. 4), MOS646 *syEx*[(*str-*

1::GCaMP3;str-1p::dsred;pha-1rescue) +(pha-1; lite-1) + him-5(e1490) + npr-5(ok1583) + him-8(e1489)](Fig. 5), MOS482 *kyEx4857*[*mod-1::GCaMP5::myo3::cherry + npr-5(ok1583) + him-8(e1489)*](Fig. 5 and Fig. S4), MOS446 *olaEx1316*[*Pttx3::CD4::GFP(11)+Pglr-3::CD4::GFP(1-10) + Pttx-3::mCherry::rab-3 + unc-122p::GFP npr-5(ok1583) + him-8(e1489)*](Fig. 5), MOS636 [*Ex(Ptax-4::npr-5 cDNA; unc-122:GFP)+him-5(e1490)*](Fig. 6)

Nematodes were cultivated on regular NGM plates on *Escherichia coli* strain OP50 at room temperature unless otherwise mentioned. *him-5*(e1490) were used as a source for wild-type males. The *Pseudomonas aeruginosa* (PA14) strain used in this study was obtained from DZMS (DSM No:19882).

PA14 aversive learning

Animals were age-synchronized by bleaching, unless otherwise specified, and were grown at room temperature on OP50 plates until they were late L4 and then separated into males and females for behavioral assays. The training and assay plates were slightly modified from [27].

Briefly, OP50 and PA14 were streaked from glycerol stocks onto LB plates and incubated at 37°C overnight. They were then moved to 4°C and used for up to a week. To prepare OP50 or PA14 cultures used in the training and assay plates, a small amount of bacteria from streaked plates were incubated in 15ml tubes containing 5ml LB at 37°C overnight at 250 rpm. After which, the specified amount of overnight culture (200µl bacteria for the training plates and 10µl for the assay plates) was plated onto dried NGM plates and incubated at 37°C overnight and then at 26°C for 24 hours. Before being used for behavioral assays, the plates were acclimatized to room temperature. Care was taken to avoid overly dried or contaminated plates. Before each experiment, a test batch of training and assay plates were verified for behavioral consistency using young adult hermaphrodites, failure of which resulted in fresh streaks from a glycerol stock.

For the training, sex-separated animals were washed using distilled water or M9 and introduced into training plates for 6 hours at room temperature unless otherwise mentioned. Excess liquid was dried with a Kim-wipe. For the choice assay, the worms were washed off the training plates and washed twice in distilled water or M9. Then, they were placed on the choice assay plates and dried with a Kim-wipe. Once dried, they were left at RT for an hour before being scored manually.

Response Index = $\frac{\#\,worms\ on\ PA14 - \#\,worms\ on\ OP50}{Total\ \#\,worms}$

Learning index = Response index$_{naïve}$ – Response index$_{trained}$

PA14 larval aversive learning

To prepare the worms, L1-arrested worms were grown on regular NGM plates until they were L3, approximately 28 hours. For the training, L3 worms were washed and put on either OP50 (control) or PA14 training plates and then incubated at RT for 6 hours. After which, they were washed off the plates and washed twice in distilled water or M9. Then, they were placed on choice assay plates and dried with a Kim-wipe. Once dried, they were left at RT for an hour and then, using a sharp surgical blade, three 1.5cm plugs from the choice areas of the plate were separated as follows: OP50 choice, PA14 choice and Indecision choice (point of insert) and plated onto respective food plates. After 24 hours, the plates were sexed to determine the ratio of each sex in the choice made.

Fast-Killing assay

The fast killing plates were prepared as described [25]. Briefly, PSG media (Peptone-Glucose-Sorbitol (1% Bacto-Peptone; 1% NaCl; 1% glucose; 0.15M sorbitol; 1.7% Bacto-Agar)) was poured onto 3cm plates and then left to dry. The bacterial cultures were prepared as described above. 10ul of the overnight culture of PA14 was then used to inoculate the plates and spread evenly using a spreader. The worms were also prepared as described above; sex-separated young adults of each sex (50-80 animals) were introduced to the killing plates and incubated at RT for 21 hours; the number of live worms was counted every 6 hours, with dead worms removed from the plates. Once tabulated, the survival percentage was calculated. The assay was done in three technical replicates.

Slow-killing assay

The slow-killing assay was based on previous methods [25] with slight modifications. The bacterial cultures and plates were prepared as described above, except 20µl of the overnight culture of PA14 was used to inoculate regular NGM plates and spread evenly using a spreader. Before introducing the worms, 40 µl of 100mM FUDR was dropped on to the sides of the plate. The worms were prepared as described above, and sex-separated young adults of each sex (40-100 animals) were introduced to the killing plates and incubated at RT for 96 hours, during which, the number of live worms was counted every 24 hours, with dead worms removed from the plates. Once tabulated, the survival percentage was calculated. The assay was done in two biological replicates.

Lawn-leaving assay

The bacterial cultures and plates were prepared as described above, except 30µl of the overnight culture of OP50 or PA14 inoculum used to inoculate normal 6 cm NGM plates. Next, sex-separated age-synchronized animals were introduced and left at RT for 6-8 hours, and then the number of worms inside or outside the lawn was counted.

IRG-1 imaging

Age-synchronized animals were incubated on OP50 or PA14 training plates for 6 hours and imaged under a Zeiss LSM 880 confocal microscope at 25x magnification on an agar pad. The PA14 groups were imaged first and the OP50 groups within 8 hours of incubation. Each image file was subjected to the same post processing by converting it to 8-bit image z-projected using maximum intensity and then subtracting background by rolling ball radius of 50 pixels and thresholded between 4-5% before selecting the Region of Interest, which ran from start of the gut until the end of the anterior region, using FIJI and the mean intensity was quantified.

AIY Rab-3 mCherry imaging

Age-synchronized animals were incubated on OP50 or PA14 training plates for 6 hours and imaged under a Zeiss LSM 880 confocal at 63x magnification on an agar pad. Each image file was subjected to the same post processing by converting it to 8-bit image, z-projected using maximum intensity and then subtracting background using rolling ball radius of 50 and thresholded to generate appropriate mask using analyze particles before selecting the Region of Interest in the red channel for mean intensity quantification. Zone 2 and Zone 3 was identified as previously described [75] and the mean intensity was quantified. To determine the delta between the training states, the males were normalized to the hermaphrodites, with hermaphrodite mean intensity taking a value of one.

Calcium imaging

Overnight cultures of OP50 and PA14 were centrifuged at 4000g for 10 minutes and the supernatant was then filtered using a 0.22-micron syringe filter. Age-synchronized animals after 6 hours of training were used for imaging. Calcium imaging was performed according to Pechuk et al. [8], with changes made to the stimulus type and duration of stimulus. Briefly, the imaging chips were fabricated according to Chronis et al. [75], with the help of the Nanofabrication Unit at the Weizmann Institute of Science. Two pumps control the flow of OP50 supernatant and PA14 supernatant into the microfluidic chip. The solutions were channeled through PVC tubes and

using a manual switch, the stimulus was presented to the worm, through stainless steel connectors. The pumping rate during experiments was ~0.005 ml/min. The worms were loaded into worm inlet of the chip by using a 1 ml syringe that had worms suspended in OP50 supernatant. 2 min habituation was given prior to imaging with the lasers on. To ensure smooth imaging, 10 mM Levamisole was added to all supernatants and 50 μM rhodamine B was added only to the PA14 supernatant to visualize stimulus delivery. Confocal imaging was done using a 40x magnification water objective. The total imaging duration was 40 sec, constituting 544 frames in total, and the stimulus duration was 12 sec for AWC, 11 sec for AWB, and 15 sec for AIY, after an equal amount of initial time to capture baseline for each neuron respectively. All imaging files were exported as tiff files and the GCaMP fluorescence intensity was analyzed using FIJI. ROIs (regions of interest) of the somas or the axon were drawn manually to best represent the signal, and their mean grey values were quantified (Data S2 for hermaphrodites, Data S3 for males). Downstream data processing was performed using MATLAB; for each worm, the baseline fluorescent level (F0) was calculated by averaging the mean grey values of 100 frames before stimulus delivery, then for each frame, the ΔF was calculated by subtracting F0 from the value of that time point, and the result was divided by F0, to normalize differences in the fluorescence baseline levels between individuals (ΔF/F0). Using the movmean function of MATLAB, the data was smoothened, and the max value in the period of interest was calculated.

Transcriptomics analysis

Approximately 700–1000 animals of each sex were subjected to PA14 or OP50 training for 6 hours and washed with M9 to remove any bacterial remnants. Each training group for each sex had 4 biological replicates. The worm pellet was flash-frozen in 500μl TRIzol using liquid nitrogen and stored at -80°C. Total RNA was extracted using the TRIzol LS (Invitrogen) protocol. The RNA from the post isopropanol precipitation step was resuspended in extraction buffer from the PicoPure (Arcturus) RNA isolation kit, and further processing was performed according to the manufacturer's recommendations.

After determining the RNA concentration, using a Qubit Fluorometer (model number 4, Invitrogen), and quality, using a Bioanalyzer (Agilent), the samples with a RIN-Score (>8) were used to create RNA-seq libraries, as previously described using the MARS-seq procedure [40]. The FASTQ files were then processed using the user-friendly transcriptome analysis pipeline (UTAP). The data thus captured was analyzed against the Wormbase database for Gene IDs.

Using Python, PCA plots were plotted using seaborn. The data was filtered by sex using the following parameters: Basemean >5 and FDR >0.05 for all analysis and genes with Basemean >5 was taken ahead for only volcano plots. The heatmaps and volcano plots were plotted using the Heatmap and EnhancedVolcano functions of R studio (2022.12.0+353), respectively. The resultant data was further taken for GO term analysis of genes from each sex (naïve vs trained) using ShinyGo [76] and the circular barplot was made using ggplot of R studio (2022.12.0+353).

Dye staining of NPR-5::GFP animals

Animals at the YA stage were washed with M9 buffer and incubated in 1ml M9 and 5µl DiD dye (Vybrant DiD Cell-labelling solution, ThermoFisher), for 1 hour, on a rotor at ~40 rpm. The worms were then transferred to food plates and the M9 allowed to dry. The animals were then sex-separated and transferred to either OP50 or PA14 training plates and incubated for 6 hours. Next, the worms were transferred to an agar pad and anesthetized with 5µl of 100mM NaN_3 and imaged under a Zeiss LSM 880 using a 40x water objective. The Region of Interest was selected in FIJI, using the DiD staining, for the positions of ASJ and AWB, while a co-injection marker was used to assess the position of AIY. The mean intensity was quantified after background correction and thresholding.

CRISPR/Cas-9 mediated *npr-5* deletion

The CRISPR strategy was based on Paix et al. [77]. Recombinant cas9 (IDT) was injected into N2 gonads with tracrRNA (IDT) and three crRNAs, one targeting the dpy-10 locus (Paix et al. 2015) and two flanking the npr-5 locus (GATAACGTTGCTGATGGTGG, located 52bp downstream of npr-5 start codon, and GAGACGGGCAAGATGAACAC, located 54bp downstream of stop codon). The repair template was the ssODN CCATTTCGACCATTTCAACCACAACGACTCCCTCCGTTCATCTTGCCCGTCTCTCGAAAAATTCCATTAT, composed of 35nt homology arms from each side of the npr-5 locus. Rol/dpy F1 progeny were screened by PCR to identify the npr-5(ety11) deletion allele. Three primers were included in the reaction: TTCGATGCATGGTTAGTTCG (npr-5 CR_F1), TTTCCATGTCACTCGTCAGC (npr-5 CR_R1), GGAAATTCCCGGAAAATGAT (npr-5 CR_R2), resulting in a 347bp band in WT animals and a 577bp band in ety11 animals.

Mated learning assay

The assay for the virgin groups was carried out as described above. However, for the mated groups, hermaphrodites were introduced into the training plates at the start of the assay, and at

the end of 6 hours, the males were separated, and the downstream processing was continued as usual.

Transgenic strains/molecular cloning

The feminization of the gut was generated by expressing *tra-2[intracellular]* under the *elt-2* promoter, using the primers as described in Table S1.

Quantification and statistical analysis

Each Figure legend contains details of the quantification, statistical tests performed and the sample sizes of each individual experiment. All statistical analysis was performed on GraphPad Prism 10. **Funding:** MOS acknowledges financial support from the European Research Council ERC-2019-STG 850784, Israel Science Foundation grant 961/21, Dr. Barry Sherman Institute for Medicinal Chemistry, Sagol Weizmann-MIT Bridge Program and the Azrieli Foundation. MOS is the incumbent of the Jenna and Julia Birnbach Family Career Development Chair.

Authors contribution: SPK conducted and analyzed the experiments. RH performed the library preparation and sequencing for the transcriptomics experiment. AG performed and analyzed the *npr-5* dye staining experiment. MOS supervised and designed the experiments. SPK and MOS wrote the paper.

Competing interests: The authors declare no competing interests.

Data and materials availability: All data used for analysis are available in the manuscript or the supplementary materials.

References

1. Mery, F. Natural variation in learning and memory. *Curr. Opin. Neurobiol.* **23**, 52–56 (2013).

2. Crossley, M., Benjamin, P. R., Kemenes, G., Staras, K. & Kemenes, I. A circuit mechanism linking past and future learning through shifts in perception. *Sci. Adv.* **9**, eadd3403 (2023).

3. Asok, A., Leroy, F., Rayman, J. B. & Kandel, E. R. Molecular Mechanisms of the Memory Trace. *Trends Neurosci.* **42**, 14–22 (2019).

4. Janicke, T., Häderer, I. K., Lajeunesse, M. J. & Anthes, N. Darwinian sex roles confirmed across the animal kingdom. *Sci. Adv.* **2**, e1500983 (2016).

5. Connallon, T. The geography of sex□specific selection, local adaptation, and sexual dimorphism. *Evolution* **69**, (2015).

6. Paletta, P., Bass, N., Aspesi, D. & Choleris, E. Sex Differences in Brain Function and Dysfunction. *Curr Top Behav Neurosci* **62**, 207–234 (2022).

7. Gall, C. M., Le, A. A. & Lynch, G. Sex differences in synaptic plasticity underlying learning. *J. Neurosci. Res.* **101**, 764–782 (2023).

8. Pechuk, V. *et al.* Reprogramming the topology of the nociceptive circuit in C. elegans reshapes sexual behavior. *Curr Biol* (2022) doi:10.1016/j.cub.2022.08.038.

9. Beck, K. D. & Luine, V. N. Evidence for sex-specific shifting of neural processes underlying learning and memory following stress. *Physiol Behav* **99**, 204–211 (2010).

10. Ehmann, B. *et al.* Immature wild orangutans acquire relevant ecological knowledge through sex-specific attentional biases during social learning. *Plos Biol* **19**, e3001173 (2021).

11. Carazo, P., Noble, D. W. A., Chandrasoma, D. & Whiting, M. J. Sex and boldness explain individual differences in spatial learning in a lizard. *Proc Royal Soc B Biological Sci* **281**, 20133275 (2014).

12. Chiu, H. *et al.* A circuit logic for sexually shared and dimorphic aggressive behaviors in Drosophila. *Cell* **184**, 507-520.e16 (2021).

13. Verzijden, M. N. *et al.* The impact of learning on sexual selection and speciation. *Trends Ecol. Evol.* **27**, 511–519 (2012).

14. Møller, A. P. The Behavior of Animals, 2nd Edition. 315–341 (2021) doi:10.1002/9781119109556.ch12.

15. Molina-García, L. & Barrios, A. Sex differences in learning—shared principles across taxa. *Curr. Opin. Physiol.* **6**, 65–74 (2018).

16. McCarthy, M. M. & Arnold, A. P. Reframing sexual differentiation of the brain. *Nature Neuroscience* **14**, 677–683 (2011).

17. Rahmani, A. & Chew, Y. L. Investigating the molecular mechanisms of learning and memory using Caenorhabditis elegans. *J. Neurochem.* **159**, 417–451 (2021).

18. Sakai, N. *et al.* A sexually conditioned switch of chemosensory behavior in C. elegans. *PLoS ONE* **8**, e68676 (2013).

19. Ghosh, D. D., Nitabach, M. N., Zhang, Y. & Harris, G. Multisensory integration in C. elegans. *Curr. Opin. Neurobiol.* **43**, 110–118 (2017).

20. Stein, G. M. & Murphy, C. T. C. elegans positive olfactory associative memory is a molecularly conserved behavioral paradigm. *Neurobiol. Learn. Mem.* **115**, 86–94 (2014).

21. Kaletsky, R. *et al.* C. elegans interprets bacterial non-coding RNAs to learn pathogenic avoidance. *Nature* **586**, 445–451 (2020).

22. Sasakura, H. & Mori, I. Behavioral plasticity, learning, and memory in C. elegans. *Curr. Opin. Neurobiol.* **23**, 92–99 (2013).

23. Setty, H. *et al.* Sexually dimorphic architecture and function of a mechanosensory circuit in C. elegans. *Biorxiv* 2022.02.18.481005 (2022) doi:10.1101/2022.02.18.481005.

24. Ryan, D. A. *et al.* Sex, age, and hunger regulate behavioral prioritization through dynamic modulation of chemoreceptor expression. *Curr Biol* **24**, 2509–2517 (2014).

25. Tan, M.-W., Mahajan-Miklos, S. & Ausubel, F. M. Killing of Caenorhabditis elegans by Pseudomonas aeruginosa used to model mammalian bacterial pathogenesis. *Proc National Acad Sci* **96**, 715–720 (1999).

26. Liu, H. *et al.* Forgetting generates a novel state that is reactivatable. *Sci Adv* **8**, eabi9071 (2022).

27. Zhang, Y., Lu, H. & Bargmann, C. I. Pathogenic bacteria induce aversive olfactory learning in Caenorhabditis elegans. *Nature* **438**, 179–184 (2005).

28. Estes, K. A., Dunbar, T. L., Powell, J. R., Ausubel, F. M. & Troemel, E. R. bZIP transcription factor zip-2 mediates an early response to Pseudomonas aeruginosa infection in Caenorhabditis elegans. *Proc National Acad Sci* **107**, 2153–2158 (2010).

29. O'Donnell, M. P., Fox, B. W., Chao, P.-H., Schroeder, F. C. & Sengupta, P. A neurotransmitter produced by gut bacteria modulates host sensory behaviour. *Nature* **583**, 415–420 (2020).

30. Singh, J. & Aballay, A. Intestinal infection regulates behavior and learning via neuroendocrine signaling. *Elife* **8**, e50033 (2019).

31. Ha, H. *et al.* Functional organization of a neural network for aversive olfactory learning in Caenorhabditis elegans. *Neuron* **68**, 1173–1186 (2010).

32. Jin, X., Pokala, N. & Bargmann, C. I. Distinct Circuits for the Formation and Retrieval of an Imprinted Olfactory Memory. *Cell* **164**, 632–643 (2016).

33. Bargmann, C. I., Hartwieg, E. & Horvitz, H. R. Odorant-selective genes and neurons mediate olfaction in C. elegans. *Cell* **74**, 515–527 (1993).

34. Troemel, E. R., Kimmel, B. E. & Bargmann, C. I. Reprogramming Chemotaxis Responses: Sensory Neurons Define Olfactory Preferences in C. elegans. *Cell* **91**, 161–169 (1997).

35. Prakash, D. *et al.* 1□Undecene from Pseudomonas aeruginosa is an olfactory signal for flight□or□fight response in Caenorhabditis elegans. *Embo J* **40**, e106938 (2021).

36. Hawk, J. D. *et al.* Integration of Plasticity Mechanisms within a Single Sensory Neuron of C. elegans Actuates a Memory. *Neuron* **97**, 356-367.e4 (2018).

37. Chandra, R. *et al.* Sleep is required to consolidate odor memory and remodel olfactory synapses. *Cell* **186**, 2911-2928.e20 (2023).

38. Satoh, Y. *et al.* Regulation of Experience-Dependent Bidirectional Chemotaxis by a Neural Circuit Switch in Caenorhabditis elegans. *J. Neurosci.* **34**, 15631–15637 (2014).

39. Colón-Ramos, D. A., Margeta, M. A. & Shen, K. Glia promote local synaptogenesis through UNC-6 (netrin) signaling in C. elegans. *Science* **318**, 103–106 (2007).

40. Jaitin, D. A. *et al.* Massively parallel single-cell RNA-seq for marker-free decomposition of tissues into cell types. *Science* **343**, 776–779 (2014).

41. Okkema, P. G. & Kimble, J. Molecular analysis of tra-2, a sex determining gene in C.elegans. *EMBO J.* **10**, 171–176 (1991).

42. Barr, M. M. & Sternberg, P. W. A polycystic kidney-disease gene homologue required for male mating behaviour in C. elegans. *Nature* **401**, 386–389 (1999).

43. Kawli, T. & Tan, M.-W. Neuroendocrine signals modulate the innate immunity of Caenorhabditis elegans through insulin signaling. *Nat Immunol* **9**, 1415–1424 (2008).

44. Yu, Y., Zhi, L., Guan, X., Wang, D. & Wang, D. FLP-4 neuropeptide and its receptor in a neuronal circuit regulate preference choice through functions of ASH-2 trithorax complex in Caenorhabditis elegans. *Sci Rep-uk* **6**, 21485 (2016).

45. Deng, P. *et al.* Mitochondrial UPR repression during Pseudomonas aeruginosa infection requires the bZIP protein ZIP-3. *Proc National Acad Sci* **116**, 6146–6151 (2019).

46. Wu, T. *et al.* Pheromones Modulate Learning by Regulating the Balanced Signals of Two Insulin-like Peptides. *Neuron* **104**, 1095-1109.e5 (2019).

47. Zheng, Z. *et al.* GABAergic synapses suppress intestinal innate immunity via insulin signaling in Caenorhabditis elegans. *Proc National Acad Sci* **118**, e2021063118 (2021).

48. Marquina-Solis, J. *et al.* Peptidergic signaling controls the dynamics of sickness behavior in Caenorhabditis elegans. *Biorxiv* 2022.04.16.488560 (2022) doi:10.1101/2022.04.16.488560.

49. Chang, H. C., Paek, J. & Kim, D. H. Natural polymorphisms in C. elegans HECW-1 E3 ligase affect pathogen avoidance behaviour. *Nature* **480**, 525–529 (2011).

50. Chen, Z. *et al.* Two Insulin-like Peptides Antagonistically Regulate Aversive Olfactory Learning in C. elegans. *Neuron* **77**, 572–585 (2013).

51. Lee, K. & Mylonakis, E. An Intestine-Derived Neuropeptide Controls Avoidance Behavior in Caenorhabditis elegans. *Cell Reports* **20**, 2501–2512 (2017).

52. Cao, X., Kajino-Sakamoto, R., Doss, A. & Aballay, A. Distinct Roles of Sensory Neurons in Mediating Pathogen Avoidance and Neuropeptide-Dependent Immune Regulation. *Cell Reports* **21**, 1442–1451 (2017).

53. Zhang, X. & Zhang, Y. DBL-1, a TGF-β, is essential for Caenorhabditis elegans aversive olfactory learning. *Proc National Acad Sci* **109**, 17081–17086 (2012).

54. Meisel, J. D., Panda, O., Mahanti, P., Schroeder, F. C. & Kim, D. H. Chemosensation of Bacterial Secondary Metabolites Modulates Neuroendocrine Signaling and Behavior of C. elegans. *Cell* **159**, 267–280 (2014).

55. Cohen, M. *et al.* Coordinated Regulation of Foraging and Metabolism in C. elegans by RFamide Neuropeptide Signaling. *Cell Metab* **9**, 375–385 (2009).

56. Bhardwaj, A., Pandey, P. & Babu, K. Control of Locomotory Behavior of Caenorhabditis elegans by the Immunoglobulin Superfamily Protein RIG-3. *Genetics* **214**, 135–145 (2020).

57. Gøtzsche, C. R. & Woldbye, D. P. D. The role of NPY in learning and memory. *Neuropeptides* **55**, 79–89 (2016).

58. Pleil, K. E. *et al.* NPY signaling inhibits extended amygdala CRF neurons to suppress binge alcohol drinking. *Nat Neurosci* **18**, 545–552 (2015).

59. Zhou, Z. *et al.* Genetic variation in human NPY expression affects stress response and emotion. *Nature* **452**, 997–1001 (2008).

60. Naveilhan, P. *et al.* Normal feeding behavior, body weight and leptin response require the neuropeptide Y Y2 receptor. *Nat Med* **5**, 1188–1193 (1999).

61. Cohen, H. *et al.* The Neuropeptide Y (NPY)-ergic System is Associated with Behavioral Resilience to Stress Exposure in an Animal Model of Post-Traumatic Stress Disorder. *Neuropsychopharmacol* **37**, 350–363 (2012).

62. Hilbert, Z. A. & Kim, D. H. Sexually dimorphic control of gene expression in sensory neurons regulates decision-making behavior in C. elegans. *Elife* **6**, 386 (2017).

63. Flavell, S. W. *et al.* Serotonin and the neuropeptide PDF initiate and extend opposing behavioral states in C. elegans. *Cell* **154**, 1023–1035 (2013).

64. Szklarczyk, D. *et al.* The STRING database in 2021: customizable protein–protein networks, and functional characterization of user-uploaded gene/measurement sets. *Nucleic Acids Res.* **49**, gkaa1074- (2020).

65. Gutiérrez-Menéndez, A., Méndez, M. & Arias, J. L. Learning and metabolic brain differences between juvenile male and female rats in the execution of different training regimes of a spatial memory task. *Physiol Behav* **267**, 114203 (2023).

66. Rama, S., Zbili, M. & Debanne, D. Signal propagation along the axon. *Curr. Opin. Neurobiol.* **51**, 37–44 (2018).

67. Morais, L. H., Schreiber, H. L. & Mazmanian, S. K. The gut microbiota–brain axis in behaviour and brain disorders. *Nat Rev Microbiol* **19**, 241–255 (2021).

68. Hamson, D. K., Roes, M. M. & Galea, L. A. M. Comprehensive Physiology. *Compr. Physiol.* **6**, 1295–1337 (2017).

69. Frick, K. M., Kim, J., Tuscher, J. J. & Fortress, A. M. Sex steroid hormones matter for learning and memory: estrogenic regulation of hippocampal function in male and female rodents. *Learn. Mem.* **22**, 472–493 (2015).

70. Ernst, D. A., Agcaoili, G. A., Merrill, A. N. & Westerman, E. L. A learning experience elicits sex□dependent neurogenomic responses in Bicyclus anynana butterflies. *Mol Ecol* (2023) doi:10.1111/mec.16920.

71. Kilpatrick, Z. P., Davidson, J. D. & Hady, A. E. Uncertainty drives deviations in normative foraging decision strategies. *J Roy Soc Interface* **18**, 20210337 (2021).

72. Wu, T. *et al.* Pathogenic bacteria modulate pheromone response to promote mating. *Nature* **613**, 324–331 (2023).

73. Manning, T. H., Austin, M. W., MuseMorris, K. & Dunlap, A. S. Equivalent learning, but unequal participation: Male bumble bees learn comparably to females, but participate in cognitive assessments at lower rates. *Behav Process* **193**, 104528 (2021).

74. Wolf, S. & Chittka, L. Male bumblebees, Bombus terrestris, perform equally well as workers in a serial colour-learning task. *Anim Behav* **111**, 147–155 (2016).

75. Chronis, N., Zimmer, M. & Bargmann, C. I. Microfluidics for in vivo imaging of neuronal and behavioral activity in Caenorhabditis elegans. *Nature Methods* **4**, 727–731 (2007).

76. Ge, S. X., Jung, D. & Yao, R. ShinyGO: a graphical enrichment tool for animals and plants. *Bioinformatics* **36**, 2628–2629 (2019).

77. Paix, A., Folkmann, A., Rasoloson, D. & Seydoux, G. High Efficiency, Homology-Directed Genome Editing in Caenorhabditis elegans Using CRISPR-Cas9 Ribonucleoprotein Complexes. *Genetics* **201**, 47–54 (2015).